Global Comparative Basin Hypsometric Analysis of Earth and Mars: Implications for Early Mars Climate

J. Fang[1], W. Luo[1], A. D. Howard[2], R. A. Craddock[3], E. A. Oliveira[4], R. S. Pires[4]

[1]Northern Illinois University, DeKalb, IL, USA

[2]Planetary Science Institute, Tucson, AZ, USA

[3]Smithsonian Institution, Washington, DC, USA

[4]University of Fortaleza, Fortaleza, Ceará, Brazil

Corresponding author: Wei Luo (wluo@niu.edu)

Key Points:

- Early Martian climate was likely more arid than hyper-arid Earth or the duration of more humid conditions on Mars was short-lived.
- Differences in some hypsometric attributes between Mars and the Moon suggest that water erosion was likely sourced from precipitation.
- Impact cratering played an important role in preconditioning the Martian surface while interfering with subsequent fluvial erosion.

Abstract

While there is a consensus that water played at least some role in the formation of various Martian landforms, including valley networks (VNs), the specific mechanisms and climate conditions are still debated. Basin hypsometric curves, reflecting elevation distributions, offer insights into past processes and climates. Our study presents a global-scale comparison of basin hypsometry on Mars, Earth, the Moon, and artificial fractal surfaces. Results indicate Martian VN formation likely occurred under a climate more arid than hyper-arid Earth, or under more humid periods that were short-lived. Differences in hypsometric attributes between Mars and the Moon suggest VN formation on Mars involved precipitation-driven water flow. Additionally, impact cratering significantly influenced Martian surface conditions, potentially disrupting fluvial erosion processes. This comparative analysis sheds light on the complex interplay of climatic factors and geological processes in Martian landscape evolution.

Plain Language Summary

Many lines of evidence suggest that water has shaped the landscapes of Mars, especially its valley networks (VNs), but exactly how this happened and what the climate was like at the time are still up for debate. Here we study and compare how basin shape changes with elevation on Mars, Earth, the Moon, and some artificial surfaces. Our findings suggest that when the VNs formed on Mars, the climate was likely drier than Earth's, or there were only brief periods of wetter conditions. We also noticed differences between Mars and the Moon, indicating that the water responsible for carving the VNs on Mars likely came from rainfall. We also found that impact cratering played a big part in shaping the Martian surface and could have messed with the way Martian valleys formed. This research helps us understand how Mars' landscapes formed and evolved over time.

1 Introduction

The current climatic conditions on Mars do not support liquid water on its surface. However, a wealth of geologic and geomorphic evidence, including the presence of valley networks (Ansan & Mangold, 2013; Hynek et al., 2010; Hynek & Phillips, 2003; Luo & Stepinski, 2009; Mangold et al., 2004), alluvial fans and deltas (Wilson et al., 2021), and paleolake sediments (Fassett & Head, 2008; Goudge et al., 2016, 2016; Rapin et al., 2019), points to the past role of water as a key agent in shaping the landscape we observe today (Craddock & Howard, 2002; Ramirez & Craddock, 2018). Valley networks (VNs), which are dendritic/linear features similar to river valleys on Earth, are widely distributed on the southern highlands of Mars, mostly in the ancient Noachian terrains (~3.7Ga). This implies that Mars was at least warm enough for some period of time to support liquid water (Craddock & Howard, 2002; Hynek & Phillips, 2003; Luo & Stepinski, 2009; Ramirez & Craddock, 2018). However, some climate models have difficulties in creating such early warm and wet conditions, mainly due to the Martian orbit that is farther away from the Sun and the faintness of the young Sun at the time when the VNs were forming (e.g., Wordsworth 2016). This has led to many debates about VN's formation processes and early Mars climatic conditions. A number of alternative hypotheses have been proposed that try to reconcile the discrepancy between climate models and geologic/geomorphic evidence. For example, the climate might have been only episodically warm and wet due to brief and intense volcanic activity with associated outgassing of greenhouse gasses and aerosols (Halevy & Head, 2014); VNs could be created by groundwater sapping associated with magma intrusion and hydrothermal activities, thus not requiring continuous warm and wet conditions (Gulick, 1998); VNs could also be carved by melt water during short-lived episodes of top-down melting of thick cold-based ice on the equatorial highlands (Fastook & Head, 2015; Forget et al., 2013; Wordsworth et al., 2013, 2015) or localized basal melting and erosion by subglacial flows (Grau Galofre et al., 2020). There appears to be a general consensus that water played at least some role in the formation VNs; however, the specifics of water's involvement and the climatic conditions still remain elusive (Baker et al., 2015; Ehlmann et al., 2011; Ramirez et al., 2020; Ramirez & Craddock, 2018; Turbet & Forget, 2019; Wordsworth, 2016).

Quantitative morphometric analysis of the landforms at basin scales can provide valuable information regarding past processes and climatic conditions. Basin hypsometry is one such morphometric analysis technique. Here we report a comprehensive global-scale comparison of hypsometric attributes of basins on Mars and Earth, along with additional basins extracted from the Moon and artificial fractal surfaces, aiming to derive a better understanding of the early Mars climate, particularly in testing whether the sources of water carving the VNs were from precipitation or other non-precipitation mechanisms such as local melting.

1.1 Previous studies on hypsometric analysis

The hypsometric curve of a basin represents the statistical distribution of elevations. It plots the relative area of the basin at or above a certain elevation to the relative elevation (Strahler, 1952). The shape of the curve reflects the development stage of the basin and erosional processes (Harlin, 1978; Luo, 2000; Strahler, 1952). Montgomery et al. (2001) qualitatively showed that hypsometry is positively correlated with climatically driven variations in geomorphologic processes across a hemisphere-scale climatic gradient of the Andes in South America. However, a more quantitative hypsometric analysis to establish the relationship between basin hypsometry and climate, especially at global scale, has not been conducted. Hypsometric curve can be treated as a cumulative probability distribution and its shape can be quantitatively characterized by statistical attributes, including hypsometric integral (HI), skewness (SK), kurtosis (KUR), density skewness (DSK), and density kurtosis (DKUR)] (Harlin, 1978; Luo, 2000, 2002). HI represents the area under the curve and it indicates the amount of erosion of the basin (the lower the HI value, the more the erosion) (Harlin, 1978; Strahler, 1952). SK depicts the asymmetry of a distribution (or how skewed the tail of the distribution is) relative to a normal distribution. Higher SK value (i.e., more positively skewed) signifies more erosion in the upper reaches of the basin (Harlin, 1978). KUR portrays the peakedness of a distribution relative to a normal distribution and it represents the erosion in both upper and lower reaches of the basin (Harlin, 1978). DSK and DKUR are the skewness and kurtosis of the density function of the distribution and they characterize the rate of basin slope change and mid-basin slope, respectively (Harlin, 1978). Two example basins (one with erosion concentrated in the lower reach of the basin, the other with headward erosion extended to the upper reach of the basin) from the original Harlin (1978) paper are reproduced in Fig. S1 to help readers understand the meaning of these attributes. The physical meaning of each attribute is summarized in Table 1 (Harlin, 1978). This study intends to compare these quantitative attributes from a spectrum of topographic surfaces to better understand the early Mars climate conditions and processes forming the VNs.

Table 1 Physical Meaning of Hypsometric Attributes[a]

Parameter	Meaning
Integral (HI)	Mass left after erosion
Skewness (SK)	Amount of erosion in the upper reach of basin
Kurtosis (KUR)	Erosion in both upper and lower reaches of basin
Density Skewness (DSK)	Rate of slope change
Density Kurtosis (DKUR)	Mid-basin slope

[a]Compiled after Harlin (1978).

2 Data and Methods

2.1 Data

The basis for conducting our study was digital elevation model (DEM) data, from which watershed boundary and hypsometric attributes were extracted. For Earth, a void-filled DEM at 3 arc-seconds resolution (approximately 90-m at the equator) from HydroSHEDS core dataset was used (Lehner & Grill, 2013). The dataset covers only 60° north and 56° south latitudes of the Earth, which represents about 80% of the earth land surface. This is sufficient for the purpose of comparing fluvial systems on Earth to VNs on Mars. In addition, Global Aridity Index (AI) and the Potential Evapotranspiration Climate Database (Zomer et al., 2022) were used for Earth climate information.

The main topographic data set for Mars was the Mars Obiter Laser Altimeter (MOLA) – High Resolution Stereo Camera (HRSC) Blended DEM (Fergason et al., 2018), with a spatial resolution of 200 m. For the Moon, we used the Lunar Orbiter Laser Altimeter (LOLA) DEM with a spatial resolution of 118 m at the equator. To examine the end member condition of a primitive surface with no geologic modification processes, we generated a number of fractal surfaces with a Hurst exponent, H, ranging from 0.05 to 0.35 (fractal dimension D = 3-H for a 3D surface, (Franceschetti & Riccio, 2007)).

2.2 Basin boundaries

Basin boundary is critical for conducting any hypsometric analysis. For Earth, there is abundant data for many watershed basin boundaries. However, for Mars and the Moon we had to extract the basin boundary from the DEM data. It has been shown in previous studies that applying the traditional flow-based algorithm for extracting watershed boundaries (e.g., the D8 algorithm) on Earth to planetary bodies can be problematic and requires many parameter tweaking (Ansan & Mangold, 2013; Mest et al., 2010; Stepinski & Coradetti, 2004), mainly due to impact craters that modified the landscape subsequent to valley network formation. Luo et al. (2023) successfully adapted the parameter-free Invasion Percolation-Based Algorithm (IPBA) (Fehr et al., 2009; Oliveira et al., 2019) to extract Martian drainage basins from mapped VNs. The IPBA algorithm is particularly suited for our purpose of extracting basin boundaries for the Moon and fractal surfaces using DEM data, because the algorithm does not assume flow of water. The Martian basin boundaries from Luo et al. (2023) was adopted, but we only included basins that have a drainage density greater than 0.003 km^{-1} (using VN data of Alemanno et al. (2018)) for analysis, because some lower density areas were complicated by lava flows (Fig. 1). To extract basin boundaries of the Moon, we first used the geomorphon method to classify the landscape into 10 types (e.g., pit, valley, ridge, etc.) based on the relative elevations of the cell under consideration and surrounding cells along the line of sight in 8 cardinal directions (Jasiewicz & Stepinski, 2013). Next, we input the local pit and valley geomorphon types as sinks to the IPBA algorithm to extract basin boundaries "draining" to those sinks. To speed up the processing, the LOLA DEM was resampled at 500 m, similar to that of the MOLA DEM, to extract the basin boundaries (but the hypsometric attributes were extracted based on original DEM resolution). Luo et al. (2023) have shown that the resulting watershed boundaries are not sensitive to different resolutions. We selected basins with a size >100 km^2 for the Moon and >100×100 cells for the fractal surfaces for analysis (Fig. 1). For Earth, Luo et al. (2023) have demonstrated that the IPBA extract boundaries are practically the same as the HydroBASINS level 6 data for the conterminous US as long as the proper stream lines are provided as sinks, so we chose HydroBASINS level 6 data for the global Earth basin boundaries (Fig. 1). The purpose of these selections is to have more meaningful comparison between these different surfaces.

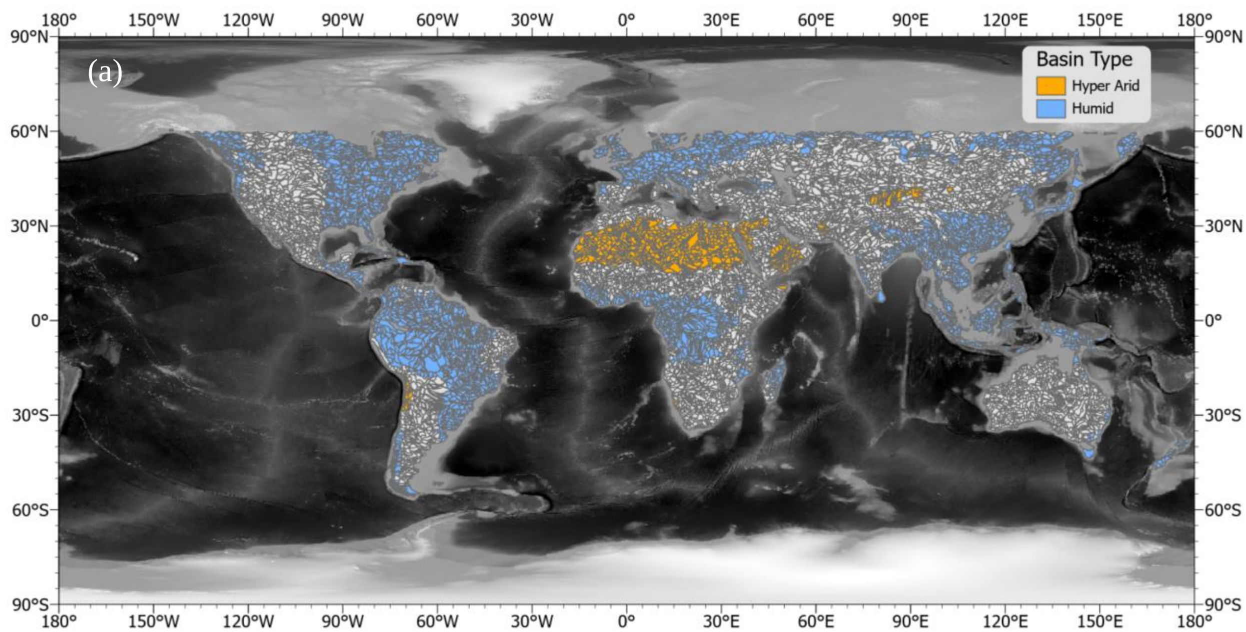

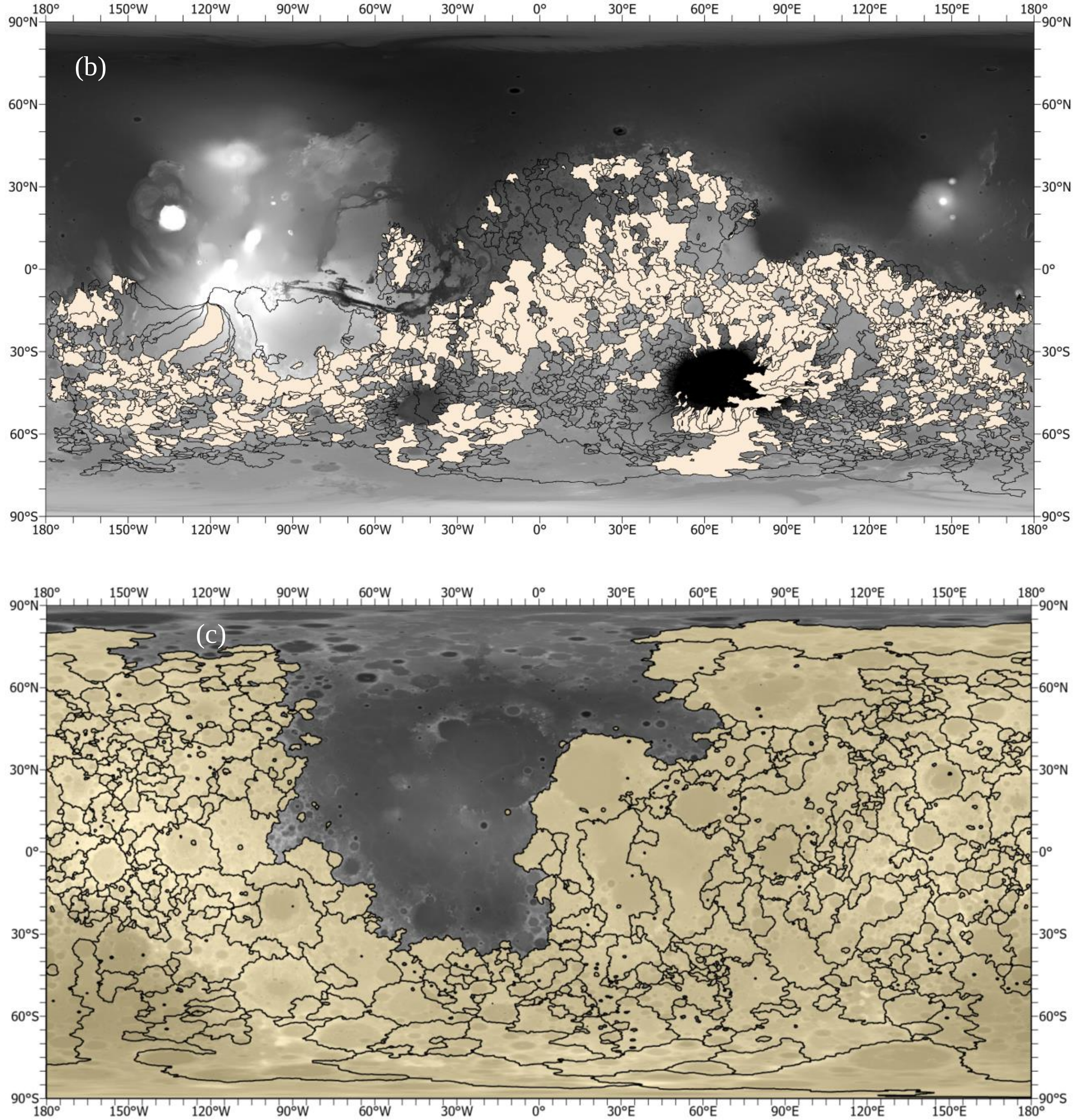

Figure 1. Basins selected for analysis: (a) terrestrial basins (separated into humid and hyper-arid basins); (b) Martian basins (filled polygons indicate selected basins, with VN density greater than 0.003 km^{-1}); (c) basins on the highland of the Moon.

2.3 Extraction of hypsometric attributes

Previous studies commonly employed the 3rd order polynomials to fit hypsometric curves and then derive hypsometric attributes based on the polynomial function (Harlin, 1978; Luo, 2000). However, it has been shown that the 3rd order polynomials may not accurately capture the hypsometric curve's intricate shape, and various alternative formulae have been proposed (Bajracharya & Jain, 2022; Liffner et al., 2018; Vanderwaal & Ssegane, 2013). Here, we adopted a 9th order polynomial function to fit the hypsometric curve, and the five statistical attributes were obtained analytically from the fitted function, thus avoiding the potential numerical errors associated with directly using unsmoothed discrete data. More details are provided in Supporting Information Text S1.

3 Results and Interpretation

3.1 General hypsometric attribute values

Fig. 2 is the boxplot of the hypsometric attributes of Earth, Mars, the Moon, and fractal surfaces. We divided Earth into humid and hyper-arid areas based on Aridity Index (AI) (Zomer et al., 2022): AI > 0.65 as humid and AI ≤0.05 as hyper-arid (UNEP, 1997). Table S1 shows the sample size and summary statistics of each surface type. Some example basins and hypsometric attributes are shown in Fig. S2. The scatter plots of hypsometric attributes for terrestrial and Martian basins are shown in Fig. S3.

<u>Observations:</u> Overall, there are general and consistent trends of HI values increasing while the other parameter values decreasing in the following order: humid Earth, hyper-arid Earth, Mars/Moon, fractal surfaces (Fig. 2). The scatter of the data also consistently decreases in the same order, with humid Earth having the most scatters and fractal surfaces the least (Fig. 2). The scatter plots (Fig. S3) also show that there are overlaps between Mars and Earth hypsometric attributes while Earth attributes are much more scattered than those of Mars. There are also some correlations between different attributes (Fig. S3).

<u>Interpretations:</u> Since HI represents the mass left after erosion (Table 1), the increasing trend of HI indicates that the amount of erosion is the largest in humid locations on the Earth (least mass left) and the least in the fractal surfaces where there is no erosion at all. This trend is likely associated with the availability of water, where the most available amounts of water would be located in humid regions on Earth while there would be no water involved at all in the fractal surfaces. This also suggests that the Martian climate during VN formation was likely more arid than hyper-arid Earth, or that the duration of more humid conditions on Mars was short-lived. The higher values of SK, KUR, DSK and DKUR for humid Earth basins than their hyper-arid counterparts are also consistent with more available water, resulting in more headward erosion (SK), more erosion in both the upper and lower reaches of the basin (KUR), higher slope change within the basin (DSK), and a higher midbasin slope (DKUR) (see Table 1). Similarly, for fractal surfaces with no water erosion at all, these last 4 hypsometric attributes have the smallest values. The values of all 5 hypsometric attributes for the Moon and Mars falling in between Earth and fractal surfaces suggest that the Moon and Mars surfaces are more eroded/modified than the primitive fractal surfaces, but not as eroded/modified as the hyper-arid Earth. The scattering of the data (Earth most, fractal surface least) is consistent with the fact that Earth is the most geologically active and dynamic planet and has undergone a multitude of erosional processes, whereas Mars and the Moon are geologically less active in comparison. The similarity in hypsometric values between Mars and the Moon may reflect the initial “pre-conditioning” by

impact cratering processes on both surfaces (Grant & Fortezzo, 2006), which is explored further below.

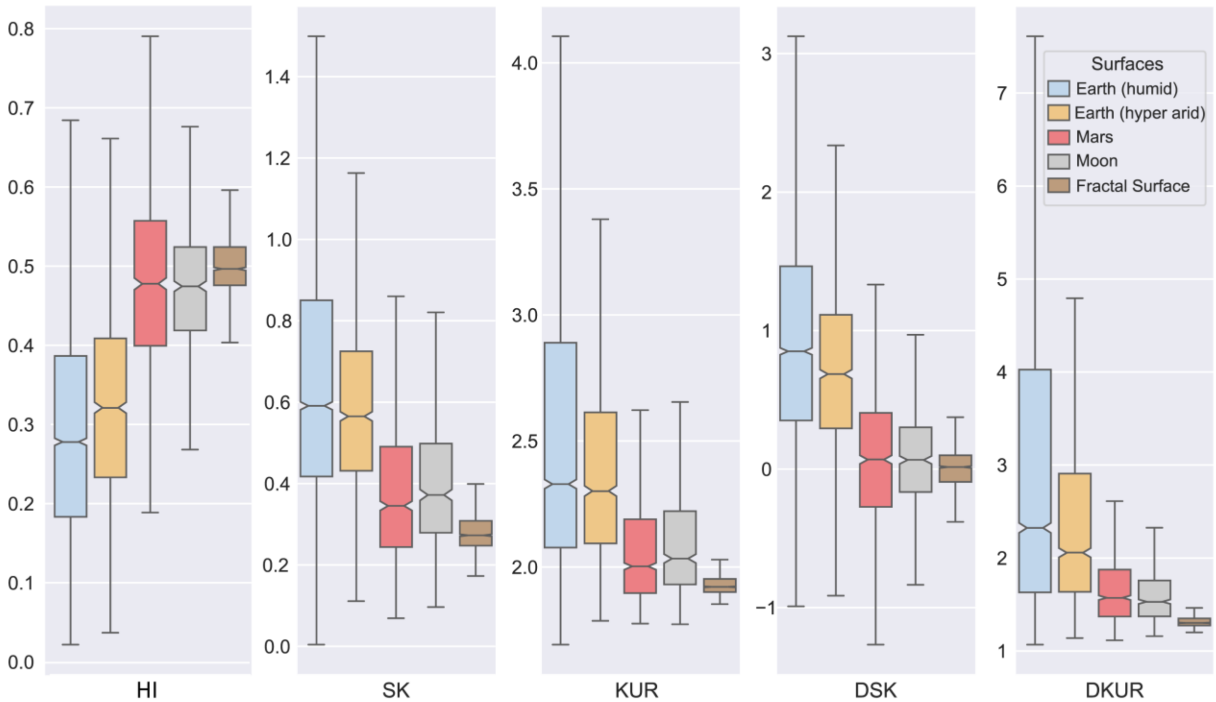

Figure 2. Boxplot of hypsometric attributes of Earth, Mars, Moon and fractal surface. (Note the vertical scales are different.)

3.2 Welch's t-test between different surfaces

To further explore the differences between all Martian basins in this study and those of other surfaces, we conducted Welch's t-test analyses. Our null hypothesis was that the hypsometric attributes are the same (assuming the variances are different). We also selected basins in regions on Mars that have high/low crater density and high/low valley density (Fig. S4) for comparison with basins on the Moon to further explore the role of impact cratering. The results are shown in Table 2 and are discussed below.

Table 2 Welch's t-tests between different groups

Row	Comparing Groups	HI	SK	KUR	DSK	DKUR
1	Hyper-arid Earth – Humid Earth	**	**	**	**	**
2	All Mars – humid Earth	**	**	**	**	**
3	All Mars – hyper-arid Earth	**	**	**	**	**
4	All Mars – Fractal	**	**	**	**	**
5	Moon – Fractal	**	**	**	**	**
6	All Mars – Moon	s	*	*	s	**

7	B(crater↑) – Moon	s	s	s	s	s
8	C(VN↓) – Moon	s	s	s	s	s
9	A(crater↓) – Moon	**	**	**	**	s
10	A(crater↓) – B(crater↑)	**	**	**	**	s
11	D(VN↑) – C(VN↓)	*	s	s	s	s
12	D(VN↑) – Moon	**	*	s	**	s
13	Model fluvial – Moon	**	**	s	s	**

**significant at 99% confidence level; *significant at 95% confidence level; s=similar (not significant) A(crater↓)=low crater density area; B(crater↑)=high crater density area; C(VN↓)=low VN density area; D(VN↑)= high VN density area.

3.2.1 Comparison to all Martian basins

Observations: The first five rows of Table 2 show the differences between humid Earth and hyper-arid Earth, all of Mars and hyper-arid Earth, all of Mars and humid Earth, all of Mars and Fractal Surfaces, and the Moon and Fractal Surfaces are all statistically significant at 99% confidence level across all hypsometric attributes. The differences between all Mars and the Moon are not significant for HI and DSK, but are significant for remaining attributes (SK, KUR, DKUR) at 95% confidence level.

Interpretations: The results in the first 5 rows of Table 2 suggest that the climatic conditions or processes responsible for modifying the different surfaces are significant and real. For example, the difference between humid and hyper-arid Earth is obviously due to water availability. The difference between Mars and hyper-arid Earth suggests that water availability also played a key role and Mars was likely more arid than the hyper-arid areas on Earth. This is consistent with previous studies (e.g., Luo et al. 2023). The differences between Mars and fractal surfaces and between the Moon and fractal surfaces can be explained by the fact that fractal surfaces have no erosion at all, whereas Mars and the Moon surface have been both modified by impact cratering and Mars likely had additional modification by water and additional processes, such as eolian and potentially glacial processes. The differences in HI and DSK between Mars and the Moon are not statistically different (Table 2 Row 6). This suggests that globally the erosion processes on Mars (fluvial and otherwise) were not significant enough to overcome signals of impact cratering, which preconditioned the initial surfaces, resulting in values of HI and DSK similar to those of the Moon. HI represents the mass left after erosion and HI alone is known to be not very diagnostic of processes (e.g., Harlin, 1978; Luo, 2000). The similar values of DSK between Mars and the Moon indicate that rate of slope change within the basins of the two planetary bodies are similar. This is consistent with findings of Grant and Fortezzo (2006), who found overall similarity of hypsometry of many basins on Mars and the Moon (independent of whether they are occupied by valleys) and similar topographic profiles between cratered basins on Mars and some fluvial basins on Earth. They interpreted the similarity as resulting from impact cratering processes that have preconfigured Martian basins for relatively efficient fluvial drainage and thus required little modification for efficient discharge of water and sediment on Mars. As discussed in the next subsection, we disagree with their last interpretation that the impact cratering makes relatively efficient drainage; on the contrary, impact cratering interferes and disrupts fluvial development, leaving surface less modified and more similar to the Moon.

However, the differences in head-ward erosion (SK), erosion in upper and lower reaches of basin (KUR), and midbasin slope (DKUR) between Mars and Moon are statistically significant (Table 2 Row 6). Considering the alternative hypotheses regarding the source of water for carving the VNs on Mars from precipitation vs melting ice/snow (e.g., Fastook & Head, 2015; Grau Galofre et al., 2020), water sourced from the atmosphere (i.e., precipitation) can explain this observation better because only precipitation can reach all parts of the basins at the same time and would make these 3 attributes different from those of the Moon. If the water is sourced from melting of ice and/or snow, the erosion would likely be concentrated more in the lower reach of the basin. This interpretation combined the earlier interpretation that Mars climate might be more arid than hyper-arid conditions on Earth suggest that early Mars climate might be overall arid but punctuated with episodic wet periods and it is during these wet periods that VNs were carved. This interpretation is also consistent with other recent studies (e.g., Cang & Luo, 2019; Luo et al., 2023).

3.2.2 Comparison using high/low crater and valley density regions on Mars

To further explore the role of impact cratering, we selected regions on Mars that have high and low crater density and valley density for comparison (see Fig. S4 for locations). For this subsection, we will describe the observation and offer our interpretations. There are no statistically significant differences between the higher crater density area (Fig. S4 Box B) on Mars and the Moon in all hypsometric attributes (Table 2 Row 7). The same is true between low VN density area (Fig. S4 Box C) on Mars and the Moon (Table 2 Row 8). This suggests that in high crater density area, the impact cratering interfered/frustrated the fluvial erosion and integration, making the erosion less effective and the resulting landscape not much different from an initial impact cratered surface (thus looking similar to the Moon surface). The low VN density area has the same effect, suggesting weak fluvial erosion does not make much difference in the impact cratering preconditioned surface.

The low crater density area (Fig. S4 Box A) is statistically different from the Moon in all parameters except DKUR (Table 2 Row 9); the same is true between low crater density (Fig. S4 Box A) and high crater density (Fig. S4 Box B) areas (Table 2 Row 10). This suggests that in low crater density area on Mars, the interference and frustration by impact cratering is less severe and thus fluvial erosion could make a significantly big difference in the initial impact cratered Martian surface.

For completeness, we also compared the high VN density area with the Moon as well as with the low VN density area. The high VN density area (Fig. S4 Box D) and low VN density area (Fig. S4 Box C) are statistically different only in HI, while similar with the rest of the hypsometric attributes (Table 2 Row 11). This can be explained by the fact that the crater density in the high VN density area (Fig. S4 Box D) is also general higher (with mean crater density value of 17.55 counts/km^2 and a standard deviation of 2.05 counts/km^2) than the low VN density area (Fig. S4 Box C, mean crater density value 6.98 counts/km^2 and standard deviation of 1.68 counts/km^2), which is also obvious visually (Fig. S4). The effect of impact cratering in the high valley network drainage density area appears to have countered many of the effects of fluvial erosion on basin hypsometry, making only the overall mass left after erosion (HI) different.

3.2.3 Comparison of simulated cratered surface and the same surface after fluvial erosion

The difference between high VN density area and the Moon are significant in HI, SK, and DSK, but insignificant in KUR and DKUR (Table 2 Row 12). To explain this, we used the MARSSIM model (Howard, 1994, 2007) to simulate cratered surfaces undergoing fluvial erosion and we ran the simulations 994 times. Two representative example outputs and their associated hypsometric curves and attributes are shown in Fig. S5. The descriptive statistics of the 994 simulations are shown in Table S1 and the Welch's t-test between the simulation and the Moon data is shown in Table 2 (Row 13). It can be seen that continuous intensive fluvial erosion on an initial cratered surface can generate significantly different hypsometric attributes (HI, SK, DKUR) from those of Moon, especially the overall erosion and precipitation that can reach the crater wall, creating the difference in HI (overall erosion) and SK (upper reach of the basin), similar to what we observe in high VN density areas on Mars (Row 12). Further modeling is needed to understand the difference/similarity in other hypsometric attributes.

4 Summary

We applied hypsometric analysis technique to Mars and Earth on a global scale and compared a set of 5 hypsometric attributes between the two planets, along with those derived from the Moon and fractal surfaces. We found a general trend of HI increasing and the rest of the hypsometric attributes decreasing in the order of humid Earth, hyper-arid Earth, Mars, the Moon and Fractal Surfaces. We interpret this trend as indicating that Mars climate was more arid than hyper-arid on Earth or that the duration of more humid conditions on Mars was short-lived. Based on the meaning of the SK, KUR, DKUR, and the fact that these 3 attributes show significant difference between Mars and the Moon, we interpret this as consistent with the VNs having been carved by water sourced from precipitation. Our results also show that impact cratering played an important role in preconditioning the Martian surface and interfering with fluvial erosion. Simulations using the MARSSIM landscape evolution model confirmed our interpretation of the role of impact cratering and the source of water coming from precipitation in explaining the basin hypsometry on Mars. However, further studies are needed to understand the full process in detail. Future work will focus on conducting more forward computer modeling using MARSSIM (Howard, 1994) to simulate the modification of the initial cratered surfaces by different erosional processes (e.g., eolian, lava flow, mass wasting) and under different climate scenarios (e.g., alternating wet and dry conditions) to see if which erosional process and scenario can produce the hypsometric attributes that best match what we observe in this study.

Acknowledgments

There are no real or perceived financial conflicts of interests for any author. This research is supported by NASA MDAP funding (award no. 80NSSC21K1087 to WL, AH, and RC and award no. 80NSSC17K0454 to RC) and Edson Queiroz Foundation (to EO and RP).

Open Research

Almost all data used in this study are publicly available and referenced. The HydroSHEDS data set (Lehner & Grill, 2013) is available at https://www.hydrosheds.org/hydrosheds-core-downloads. The Global Aridity Index and Potential Evapotranspiration Climate Database (Zomer et al., 2022) is available at https://doi.org/10.6084/m9.figshare.7504448.v4. The HRSC and MOLA Blended Digital Elevation Model (Fergason et al., 2018) is available at https://astrogeology.usgs.gov/search/map/Mars/Topography/HRSC_MOLA_Blend/Mars_HRSC_MOLA_BlendDEM_Global_200mp_v2. The Moon LRO LOLA DEM at 118m (Smith et al., 2010) is available at https://astrogeology.usgs.gov/search/details/Moon/LRO/LOLA/Lunar_LRO_LOLA_Global_LDEM_118m_Mar2014. The MARSSIM (Howard, 1994) model can be downloaded at https://csdms.colorado.edu/wiki/Model:MARSSIM.

The IPBA software code is available on GitHub (https://github.com/erneson/IPBA). The computer code for processing the data will be made available in GitHub at the publication time.

References

Alemanno, G., Orofino, V., & Mancarella, F. (2018). Global Map of Martian Fluvial Systems: Age and Total Eroded Volume Estimations. *Earth and Space Science*, *5*(10), 560–577. https://doi.org/10.1029/2018EA000362

Ansan, V., & Mangold, N. (2013). 3D morphometry of valley networks on Mars from HRSC/MEX DEMs: Implications for climatic evolution through time. *Journal of Geophysical Research: Planets*, *118*(9), 1873–1894. https://doi.org/10.1002/jgre.20117

Bajracharya, P., & Jain, S. (2022). Hydrologic similarity based on width function and hypsometry: An unsupervised learning approach. *Computers & Geosciences, 163,* 105097. https://doi.org/10.1016/j.cageo.2022.105097

Baker, V. R., Hamilton, C. W., Burr, D. M., Gulick, V. C., Komatsu, G., Luo, W., et al. (2015). Fluvial geomorphology on Earth-like planetary surfaces: A review. *Geomorphology, 245,* 149–182. https://doi.org/10.1016/j.geomorph.2015.05.002

Cang, X., & Luo, W. (2019). Noachian climatic conditions on Mars inferred from valley network junction angles. *Earth and Planetary Science Letters, 526*, 115768. https://doi.org/10.1016/j.epsl.2019.115768

Craddock, R. A., & Howard, A. D. (2002). The case for rainfall on a warm, wet early Mars. *Journal of Geophysical Research, 107(E11)*, Doi:10.1029/2001je001505.

Ehlmann, B. L., Mustard, J. F., Murchie, S. L., Bibring, J.-P., Meunier, A., Fraeman, A. A., & Langevin, Y. (2011). Subsurface water and clay mineral formation during the early history of Mars. *Nature*, *479*(7371), 53–60. https://doi.org/10.1038/nature10582

Fassett, C. I., & Head, J. W. (2008). Valley network-fed, open-basin lakes on Mars: Distribution and implications for Noachian surface and subsurface hydrology. *Icarus*, *198*(1), 37–56. https://doi.org/10.1016/j.icarus.2008.06.016

Fastook, J. L., & Head, J. W. (2015). Glaciation in the Late Noachian Icy Highlands: Ice accumulation, distribution, flow rates, basal melting, and top-down melting rates and patterns. *Planetary and Space Science, 106,* 82–98. https://doi.org/10.1016/j.pss.2014.11.028

Fehr, E., Andrade Jr, J. S., da Cunha, S. D., da Silva, L. R., Herrmann, H. J., Kadau, D., et al. (2009). New efficient methods for calculating watersheds. *Journal of Statistical Mechanics: Theory and Experiment*, *2009*(09), P09007. https://doi.org/10.1088/1742-5468/2009/09/P09007

Fergason, R. L., Hare, T. M., & Laura, J. (2018). HRSC and MOLA Blended Digital Elevation Model at 200m v2. Retrieved from http://bit.ly/HRSC_MOLA_Blend_v0

Forget, F., Wordsworth, R., Millour, E., Madeleine, J.-B., Kerber, L., Leconte, J., et al. (2013). 3D modelling of the early martian climate under a denser CO2 atmosphere: Temperatures and CO2 ice clouds. *Icarus*, *222*(1), 81–99. https://doi.org/10.1016/j.icarus.2012.10.019

Franceschetti, G., & Riccio, D. (2007). CHAPTER 3 - Surface Fractal Models. In G. Franceschetti & D. Riccio (Eds.), *Scattering, Natural Surfaces, and Fractals* (pp. 61–113). Burlington: Academic Press. https://doi.org/10.1016/B978-012265655-2/50003-9

Goudge, T. A., Fassett, C. I., Head, J. W., Mustard, J. F., & Aureli, K. L. (2016). Insights into surface runoff on early Mars from paleolake basin morphology and stratigraphy. *Geology*, *44*(6), 419–422. https://doi.org/10.1130/G37734.1

Grant, J. A., & Fortezzo, C. (2006). The evolution of Martian drainage basin hypsometry. Presented at the Lunar and Planetary Science XXXVII (2006), Houston, TX. Retrieved from https://www.lpi.usra.edu/meetings/lpsc2006/pdf/1393.pdf

Grau Galofre, A., Jellinek, A. M., & Osinski, G. R. (2020). Valley formation on early Mars by subglacial and fluvial erosion. *Nature Geoscience*, *13*(10), 663–668. https://doi.org/10.1038/s41561-020-0618-x

Gulick, V. C. (1998). Magmatic intrusions and a hydrothermal origin for fluvial valleys on Mars. *Journal of Geophysical Research*, *103*, 19,365-19,387.

Halevy, I., & Head, J. W. (2014). Episodic warming of early Mars by punctuated volcanism. *Nature Geoscience*, *7*(12), 865–868. https://doi.org/10.1038/ngeo2293

Harlin, J. M. (1978). Statistical Moments of the Hypsometric Curve and its density function. *Mathematical Geology*, *10 (1)*, 59–72.

Howard, A. D. (1994). A detachment-limited model of drainage basin evolution. *Water Resources Research*, *30*, 2261–2286.

Howard, A. D. (2007). Simulating the development of martian highland landscapes through the interaction of impact cratering, fluvial erosion, and variable hydrologic forcing. *Geomorphology*, *91*, 332–363. https://doi.org/doi:10.1016/j.geomorph.2007.04.017

Hynek, B. M., & Phillips, R. J. (2003). New data reveal mature, integrated drainage systems on Mars indicative of past precipitation. *Geology*, *31*, 757–760.

Hynek, B. M., Beach, M., & Hoke, M. R. T. (2010). Updated global map of Martian valley networks and implications for climate and hydrologic processes. *Journal of Geophysical Research-Planets*, *115*.

Jasiewicz, J., & Stepinski, T. F. (2013). Geomorphons — a pattern recognition approach to classification and mapping of landforms. *Geomorphology*, *182*, 147–156. https://doi.org/10.1016/j.geomorph.2012.11.005

Lehner, B., & Grill, G. (2013). Global river hydrography and network routing: baseline data and new approaches to study the world's large river systems: GLOBAL RIVER HYDROGRAPHY AND NETWORK ROUTING. *Hydrological Processes*, *27*(15), 2171–2186. https://doi.org/10.1002/hyp.9740

Liffner, J. W., Hewa, G. A., & Peel, M. C. (2018). The sensitivity of catchment hypsometry and hypsometric properties to DEM resolution and polynomial order. *Geomorphology*, *309*, 112–120. https://doi.org/10.1016/j.geomorph.2018.02.022

Luo, W. (2000). Quantifying groundwater sapping processes with a hypsometric analysis technique. *Journal of Geophysical Research, Planets*, 1685–1694.

Luo, W. (2002). Hypsometric Analysis of Margaritifer Sinus and Origin of Valley Networks. *Journal of Geophysical Research – Planets*, *107*, 1-1\textasciitilde1-10.

Luo, W., & Stepinski, T. F. (2009). Computer-generated global map of valley networks on Mars. *Journal of Geophysical Research-Planets*, *114*.

Luo, W., Howard, A. D., Craddock, R. A., Oliveira, E. A., & Pires, R. S. (2023). Global Spatial Distribution of Hack's Law Exponent on Mars Consistent With Early Arid Climate. *Geophysical Research Letters*, *50*(6), e2022GL102604. https://doi.org/10.1029/2022GL102604

Mangold, N., Quantin, C., Ansan, V., Delacourt, C., & Allemand, P. (2004). Evidence for Precipitation on Mars from Dendritic Valleys in the Valles Marineris Area. *Science*, *305*(5680), 78–81. https://doi.org/10.1126/science.1097549
Mest, S. C., Crown, D. A., & Harbert, W. (2010). Watershed modeling in the Tyrrhena Terra region of Mars. *Journal of Geophysical Research*, *115*(E9). https://doi.org/10.1029/2009JE003429
Montgomery, D. R., Balco, G., & Willett, S. D. (2001). Climate, tectonics, and the morphology of the Andes. *Geology*, *29*(7), 579. https://doi.org/10.1130/0091-7613(2001)029\textless0579:CTATMO\textgreater2.0.CO;2
Oliveira, E. A., Pires, R. S., Oliveira, R. S., Furtado, V., Herrmann, H. J., & Andrade, J. S. (2019). A universal approach for drainage basins. *Scientific Reports*, *9*(1), 9845. https://doi.org/10.1038/s41598-019-46165-0
Ramirez, R. M., & Craddock, R. A. (2018). The geological and climatological case for a warmer and wetter early Mars. *Nature Geoscience*, *11*(4), 230–237. https://doi.org/10.1038/s41561-018-0093-9
Ramirez, R. M., Craddock, R. A., & Usui, T. (2020). Climate Simulations of Early Mars With Estimated Precipitation, Runoff, and Erosion Rates. *Journal of Geophysical Research: Planets*, *125*(3). https://doi.org/10.1029/2019JE006160
Rapin, W., Ehlmann, B. L., Dromart, G., Schieber, J., Thomas, N. H., Fischer, W. W., et al. (2019). An interval of high salinity in ancient Gale crater lake on Mars. *Nature Geoscience*. https://doi.org/10.1038/s41561-019-0458-8
Smith, D. E., Zuber, M. T., Neumann, G. A., Lemoine, F. G., Torrence, M. H., McGarry, J. F., Rowlands, D. D., et al. (2010). Initial observations from the Lunar Orbiter Laser Altimeter (LOLA). Geophysical Research Letters, 37(18). https://doi.org/10.1029/2010GL043751
Stepinski, T. F., & Coradetti, S. (2004). Comparing morphologies of drainage basins on Mars and Earth using integral-geometry and neural maps (DOI 10 1029/2004GLO20359). *GEOPHYSICAL RESEARCH LETTERS*, *31*, n.
Strahler, A. N. (1952). Hypsometric (area- altitude) analysis of erosional topography. *Bulletin of the Geological Society of America*, *63*, 1117–1142.
Turbet, M., & Forget, F. (2019). The paradoxes of the Late Hesperian Mars ocean. *Scientific Reports*, *9*(1). https://doi.org/10.1038/s41598-019-42030-2
UNEP, (United Nations Environment Programme). (1997). World Atlas of Desertification: Second Edition. Retrieved from https://wedocs.unep.org/20.500.11822/30300
Vanderwaal, J. A., & Ssegane, H. (2013). Do Polynomials Adequately Describe the Hypsometry of M onadnock Phase Watersheds? *JAWRA Journal of the American Water Resources Association*, *49*(6), 1485–1495. https://doi.org/10.1111/jawr.12089
Wilson, S. A., Morgan, A. M., Howard, A. D., & Grant, J. A. (2021). The Global Distribution of Craters With Alluvial Fans and Deltas on Mars. *Geophysical Research Letters*, *48*(4), e2020GL091653. https://doi.org/10.1029/2020GL091653
Wordsworth, R. D. (2016). The Climate of Early Mars. *Annual Review of Earth and Planetary Sciences*, *44*(1), 381–408. https://doi.org/10.1146/annurev-earth-060115-012355
Wordsworth, R. D., Forget, F., Millour, E., Head, J. W., Madeleine, J.-B., & Charnay, B. (2013). Global modelling of the early martian climate under a denser CO2 atmosphere: Water cycle and ice evolution. *Icarus*, *222*(1), 1–19. https://doi.org/10.1016/j.icarus.2012.09.036
Wordsworth, R. D., Kerber, L., Pierrehumbert, R. T., Forget, F., & Head, J. W. (2015). Comparison of “warm and wet” and “cold and icy” scenarios for early Mars in a 3-D climate

model. *Journal of Geophysical Research: Planets*, *120*(6), 1201–1219. https://doi.org/10.1002/2015JE004787
Zomer, R. J., Xu, J., & Trabucco, A. (2022). Version 3 of the Global Aridity Index and Potential Evapotranspiration Database. *Scientific Data*, *9*(1), 409. https://doi.org/10.1038/s41597-022-01493-1